Solid State Nuclear Magnetic Resonance 34 (2008) 186–190

Contents lists available at ScienceDirect

Solid State Nuclear Magnetic Resonance

journal homepage: www.elsevier.com/locate/ssnmr

Prediction of ^{207}Pb NMR parameters for the solid ionic lead(II) halides using the relativistic ZORA-DFT formalism: Comparison with the lead-containing molecular systems

O. Dmitrenko, Shi Bai, C. Dybowski *

Department of Chemistry and Biochemistry, University of Delaware, Newark, DE 19716, USA

ARTICLE INFO

Article history:
Received 3 June 2008
Received in revised form
13 August 2008
Available online 30 August 2008

Keywords:
Nuclear magnetic resonance
NMR
Lead
Lead chloride
Lead iodide
Lead bromide
Lead fluoride
Chemical shielding
Chemical shift
Calculation
DFT
ZORA
Spin–orbit
Paramagnetic
Diamagnetic
Relativistic

ABSTRACT

Density functional calculations of ^{207}Pb NMR shielding in PbX_2 (X = F, Br, Cl and I) anionic fragments suggest that in solid PbX_2, the observed variation of chemical shift with halide is dominated by the paramagnetic contribution to the chemical shielding, with a lesser effect by the spin–orbit contribution. The calculations include relativistic effects at the level of the zero-order regular approximation (ZORA). The present observation contrasts with previous calculations for the molecular system, PbX_4, in which the spin–orbit contribution has been shown to be the major factor in the variation of the NMR chemical shift.

1. Introduction

The chemistry of solid lead compounds is complex and rich, with the element exhibiting various valence states and a variety of structural motifs. The major technological applications of lead-containing materials in batteries, thin-film capacitors and semiconducting devices [1–3] notwithstanding, the recent focus has been on the effects of lead on health and the ubiquity of lead materials in the environment, with an emphasis on removal and disposal [4,5]. Thus, understanding the chemistry of lead and its solid materials addresses a number of technological and social problems.

NMR spectroscopy provides detailed information on geometric and electronic structure for a wide variety of nuclei including ^{207}Pb [6–15]. An isotropic chemical-shift range of at least 10,000 ppm makes the ^{207}Pb NMR chemical shift a sensitive reporter of local state [11]. For solid materials, the principal values of the chemical-shift tensor vary widely from site to site, showing the striking dependence of the chemical shielding on local structure [11–13,15]. The isotropic chemical shift has been empirically correlated with other structural parameters such as interatomic distance [12] or electronegativity difference between lead and atoms in its first co-ordination sphere [9c,11]. Thus, NMR spectroscopy of lead-containing solids provides a valuable means of analyzing chemical state and structure.

The values of NMR parameters obtained from computational studies of the electronic state give insight into the nature of the connection between NMR parameters and electronic structure, allowing one to infer electronic properties from the values of NMR properties. Computation of the electronic state of a heavy nucleus such as Pb requires methods that account for the fact that electrons in these materials are relativistic particles. In this paper, we report density functional theory (DFT) calculations of the chemical-shift parameters [isotropic shift relative to

* Corresponding author. Fax: +1 302 831 6335.
E-mail address: dybowski@udel.edu (C. Dybowski).

0926-2040/$ - see front matter © 2008 Elsevier Inc. All rights reserved.
doi:10.1016/j.ssnmr.2008.08.003

tetramethyllead (TML), span (Ω) and skew (κ)] of PbX_2 (X = F, Br, Cl, I) fragments. The computational method incorporates relativistic effects through the zero-order regular approximation (ZORA) to a two-component relativistic Hamiltonian and includes spin–orbit coupling effects [16,17]. The predicted chemical shifts are in semi-quantitative agreement with experimental parameters for the solid lead(II) dihalides. The comparison of these calculations with similar calculations for lead in molecular Pb(IV) halides [16–19] demonstrates that different contributions to the chemical shielding dominate the observed trend of variation of the chemical shift with halide partner.

2. Computational methods and models

Relativistic spin–orbit ZORA-DFT calculations were performed using the Amsterdam Density Functional (ADF) program package [20] and the associated NMR program module [21,22]. The module DIRAC was applied to generate the core potentials for all atom types. Shielding-tensor calculations employed the all-electron ZORA triple-zeta basis with a double set of the polarization functions, TZ2P. We used the local density approximation (LDA) of Vosko, Wilk and Nusair (VWN) [23], augmented with the Becke88-Perdew86 generalized gradient approximation (GGA) (BP86) facility [24,25].

Calculations were performed on model anionic fragments representing the local structures. The model structures were generated from crystallographic data taken from the Inorganic Crystal Structure Database (ICSD) [26], (see Table 1) in an approach conceptually similar to a recent ^{139}La NMR computational study of the solid lanthanum (II) halides [27]. To the extent that long-range interactions do not influence the chemical shielding, calculations on fragments should provide an adequate model of the effects of structure on the chemical shielding [27].

Table 1
Calculated NMR parameters of ionic cluster PbX_2 (X = F, Br, Cl and I)

ICSD #	Model fragment	Ω (ppm)	δ_{iso} (ppm)	κ
PbF_2				
Experimental		**470**	**−2666.4**	**0.58**
14324	$[PbF_9]^{7-}$	317.2	−3076.1	0.42
$PbCl_2$				
Experimental		**533**	**−1714.9**	**0.52**
81976	$[PbCl_9]^{7-}$	561.4	−2061.3	−0.47
43344	$[PbCl_9]^{7-}$	531.9	−1832.5	0.94
15806	$[PbCl_9]^{7-}$	580.2	−1864.4	0.59
202130	$[PbCl_9]^{7-}$	620.7	−1854.0	0.37
27736	$[PbCl_9]^{7-}$	622.8	−1864.5	0.38
$PbBr_2$				
Experimental		**699**	**−980.7**	**0.58**
36170	$[PbBr_9]^{7-}$	880.1	−531.9	0.50
202134	$[PbBr_9]^{7-}$	819.8	−527.2	0.86
PbI_2				
Experimental		–[a]	**−29.1**	–[a]
42013	$[PbI_6]^{4-}$	2.4	780.3	−0.89
23762	$[PbI_6]^{4-}$	3.2	725.4	0.94
77324	$[PbI_6]^{4-}$	17.5	559.3	0.98
42510	$[PbI_6]^{4-}$	35.3	482.6	0.99
52370	$[PbI_6]^{4-}$	36.5	433.3	0.99
77325	$[PbI_6]^{4-}$	194.4	76.1	0.99
30347	$[PbI_6]^{4-}$	476.5	−62.4	0.99

[a] The experimental spectra do not allow one to specify a span for PbI_2, but from the width of the resonance, the span for PbI_2 must be less than 100 ppm. From the point group symmetry of the PbI_6^{4-} moiety, $|\kappa| = 1$. Truncation errors in the Pb–I distances result in some values deviating from this value.

NMR parameters are reported as chemical shifts relative to TML by the following relationship:

$$\delta = \frac{\sigma_{TML} - \sigma}{1 - \sigma_{TML}}. \quad (1)$$

The calculation of the ^{207}Pb NMR chemical shielding for TML was carried out within the same theory, using its experimental geometry [28], and was calculated to be 7505.662 ppm relative to the bare lead nucleus. Because of the tetrahedral symmetry, the chemical shielding of TML is isotropic, with no span or skew.

In general, the description of the resonance requires three principal values ($\delta_{11} > \delta_{22} > \delta_{33}$) of the chemical-shift tensor δ, and the orientation of the corresponding principal axes relative to a crystal-fixed co-ordinate system. From a powder spectrum, only the three principal values can be uniquely determined. It is convenient to specify three other parameters [29], the isotropic chemical shift δ_{iso}, the span Ω, and the skew κ

$$\delta_{iso} = \tfrac{1}{3}(\delta_{11} + \delta_{22} + \delta_{33}), \quad (2)$$

$$\Omega = \delta_{11} - \delta_{33}, \quad (3)$$

$$\kappa = \frac{3(\delta_{22} - \delta_{iso})}{\Omega}. \quad (4)$$

In this paper, the NMR results are given in this set of parameters.

In addition to the calculations on anionic fragments, we repeated the recent calculations for PbX_4 (X = Cl, Br and I) by Rodriguez-Fortea et al. [30], using their reported geometries and similar methods. Since our present results for PbX_4 and PbX_2 were carried out with exactly the same method, one may compare the results. Our calculations of the isotropic chemical shifts of PbX_4 are close to the previously reported values [30]. The spans for PbX_4 are essentially zero, in line with the expectations for Pb in a position of tetrahedral symmetry.

3. Results and discussion

Table 1 gives the calculated ^{207}Pb NMR parameters for each fragment structure representative of the local environment of one of the lead dihalides. The scatter in the values for a particular dihalide results from different structural parameters reported in the ICSD. In general, the calculated isotropic chemical shifts reproduce the experimental trend of increasing isotropic shielding

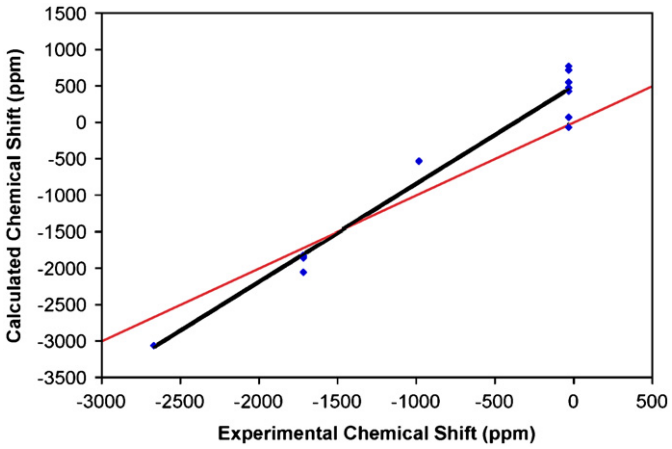

Fig. 1. A comparison of the calculated and experimental [10] isotropic chemical shifts for the lead dihalides, PbX_2 (X = F, Cl, Br, I). The shifts are referenced to the isotropic chemical shift of tetramethyllead. Multiple points indicate different reported crystal structures. The black line is the best linear fit; it has a slope of 1.3. The red line indicates the line of absolute agreement.

as the ion partner goes from I^- to Br^- to Cl^- to F^- [7,10] (Fig. 1). The calculated isotropic shifts are in semi-quantitative agreement with experimental observations, as we have previously reported [31]. It is clear that the calculated values of isotropic chemical shift are extremely sensitive to structural parameters of the model. For example, the predicted isotropic shifts of the fragment representing PbI_2 range over several hundred ppm, depending on the structural parameters chosen for the fragment. A similar, although less pronounced, variation of the isotropic shift of the fragment representing $PbCl_2$ appears in Fig. 1, as well.

The calculated spans for the various dihalide models are qualitatively in agreement with experimental observations, but again there is a spread of values for each material as a result of the spread in the X-ray structural parameters. The calculated spans for $PbCl_2$ and $PbBr_2$ are consistently larger than the experimental spans, no matter which structure is used to generate the geometry for calculation. The span for the fragment representing PbF_2 is of the order of the observed value, but it is smaller than the experimentally measured span. The situation for PbI_2 is muddled by the fact that the experimental result only indicates that the span is <100 ppm [10]. In addition, the wide range of structural parameters for PbI_2 results is a spread of values. However, with the exception of two structures, the calculations predict the span to be quite small.

Calculated skews for model clusters are given in Table 1, along with the experimental skews for the dihalides. There is variability in the calculated skew with model, as can be seen for the various models of $PbCl_2$. With some exceptions, the skews for PbF_2, $PbCl_2$, and $PbBr_2$ are generally in qualitative agreement with the experimental values, usually within ± 0.20. The skew is indicative of local point symmetry. For example, the variation in skew of the models of $PbCl_2$ can be traced to slight differences in Pb–Cl distances that change the local point symmetry.

The calculated NMR parameters of Table 1 are sensitive to slight structural differences in the model clusters. Variations in internuclear distances and/or angles between internuclear vectors may change the calculated NMR parameters by hundreds of ppm, as we have previously discussed for the isotropic shift of the $[PbI_6]^{4-}$ cluster [31]. The span also shows a range of values that depend on structural parameters such as interatomic distances. In part, this variation with structure reflects the tremendous sensitivity of the NMR measurement, but it also may indicate a limitation of using cluster models to evaluate the NMR parameters of solids.

To put the deviations of calculations from experimental results into context, a deviation between the calculated and measured shielding of 100 ppm corresponds, for a typical lead material, to approximately 1–1.5% error in predicting the shielding. The experimental measurement is typically 100 times more precise. Hence, the seemingly "large" deviations of the calculated shifts from the experimental ones demonstrate the tremendous sensitivity of the measurement, but the calculation is quite precise—in absolute terms.

The red line in Fig. 1 shows the predicted behavior for exact agreement between calculated and experimental isotropic chemical shifts of the dihalides. Even taking into account the somewhat large scatter of points due to differences in reported crystal structures, there is a systematic deviation of the data from this relationship. The average deviation over all points is 294 ppm. This average deviation indicates an average error in the calculation of the shielding of ~4%. Most of the deviation is due to the scatter for the large number of fragments of different structures representing PbI_2. The slope of the best-fit line to all data, shown in black on Fig. 1, is 1.3, not 1.0.

The total set is unusually skewed by the large number of structures for PbI_6^{4-} and $PbCl_9^{8-}$. Arbitrarily reducing the data for these two sets to the two points closest to the experimental result gives a strong linear correlation with a slope of 1.16 ($R^2 = 0.96$), closer to the expected value of 1. At this point, we cannot say whether the systematic error is a result of structural truncation or if it is inherent to the DFT calculation.

The calculations for ionic fragments PbX_n^{m-} representing the dihalides can be compared with similar calculations for the isolated lead-containing molecular systems, PbX_4 (X = Cl, Br and I), as have been reported in Ref. [30]. The results of our calculations of the isotropic shifts for the PbX_4 structures are given in Table 2, along with the values from reference [30] and experimental values. As expected for tetrahedral structures, the calculated spans are essentially zero, with no skew.

The paramagnetic contribution to the chemical shielding in the PbX_4 series is reported to decrease with the decrease of electronegativity of X, from Cl to I, but the dominant, trend-setting effect is an increase of the spin–orbit contribution, as shown in Fig. 2. Because of this trend, the isotropic chemical shift of PbX_4 correlates well with the HOMO–LUMO energy gap for PbX_4 [29]. The change in the energy gap is mostly due to a significant lowering of the HOMO ($1t_1$) energy in going from X = I to Cl in these materials.

The computed chemical shieldings for the ionic models of PbX_2 (Fig. 3) show a very different result from those of the molecular PbX_4 structures. The paramagnetic contribution in the ionic models becomes more negative as one changes the partner from F to I, which is similar to the variation of the paramagnetic contribution for the molecular PbX_4 structures. The spin–orbit contribution for PbX_2, however, decreases in going from F to I,

Table 2
NMR isotropic shifts of isolated molecules PbX_4 (X = Br, Cl and I)

Molecule	Geometry	δ_{iso} (ppm)
$PbCl_4$	Experimental[a]	−776.7
$PbCl_4$	Calculated[b]	−721.6
$PbCl_4$	Calculated[c]	−703.2
$PbBr_4$	Calculated[b]	−4824.9
$PbBr_4$	Calculated[c]	−4478.6
PbI_4	Calculated[b]	−7241.3
PbI_4	Calculated[c]	−6641.3

[a] Calculated from data of Refs. [32,33].
[b] Ref. [30].
[c] This work, based on the geometry reported in Ref. [30].

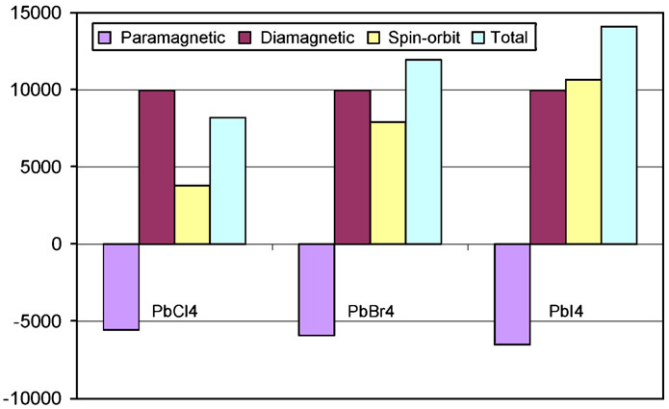

Fig. 2. The contributions to the calculated chemical shielding in molecular PbX_4 (X = Cl, Br, I).

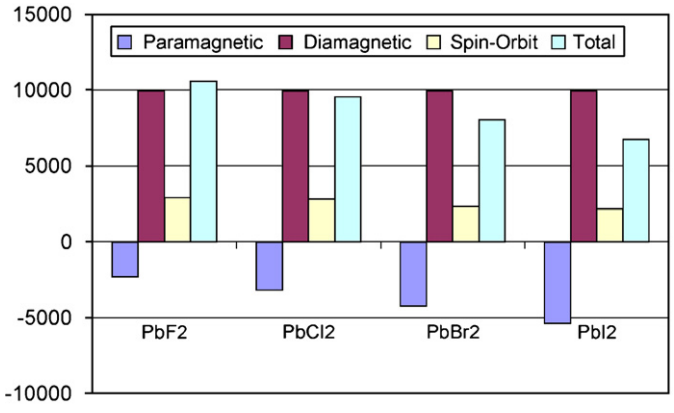

Fig. 3. The contributions to the calculated isotropic chemical shielding in fragments representing PbX_2 (X = I, Br, Cl).

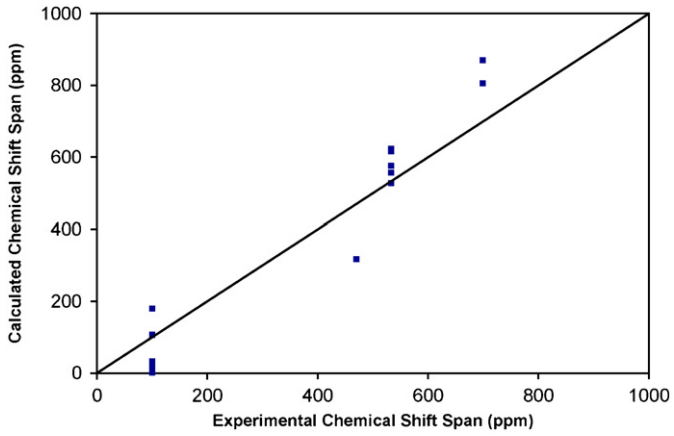

Fig. 4. A plot of the calculated span for various structures versus the experimental span for PbI_2, $PbBr_2$, and $PbCl_2$. The experimental span of PbI_2 is estimated as 100 ppm; the calculation for PbF_2 with a span of zero is left off this plot as anomalous.

which is exactly the reverse of the change for PbX_4. As a result of this inversion of the trend between PbX_4 and PbX_2, the predicted variation of the total chemical shielding of PbX_2 with counterion is opposite to that of PbX_4. It has been proposed, on the basis of nonrelativistic calculations, that this trend is a reflection of the growth of the paramagnetic contribution [7,10], but the present calculations show that the observed trend is the result of the fact that, for PbX_2, the spin–orbit contribution for PbX_2 does not vary as it does for PbX_4.

The spin–orbit contribution makes a sizable contribution to the total shielding of both PbX_2 and PbX_4, but the variation with counterion is opposite in these two cases. Large spin–orbit contributions to the chemical shielding require strong s-type bonding [30]. For ionic fragments with relatively large Pb–X distances, the relatively small values of the computed NMR spin–orbit contribution suggest that bonding does not involve s-type interactions as strongly as in the model PbX_4 structures, and that s-type bonding becomes less important for the heavier halides.

A comparison of the calculated spans of PbX_2 with the experimental results is given in Fig. 4. As with the isotropic chemical shift, the calculated span significantly deviates from the experimental span, with typical deviations from the experimental value of 15–25%. The scatter in this plot indicates the sensitivity of this parameter to the structural parameters for the model. Even with these relatively large discrepancies between experimental and calculated spans, the trend of the span with anion is qualitatively reproduced by these relativistic cluster calculations (Fig. 4), suggesting that the NMR parameters may be used to define the electronic state.

For near-octahedral structures such as PbI_6^{4-} (Fig. 5), the total span reflects the deviation, θ, of the structure from perfect octahedral symmetry (Fig. 6) [31]. One may ask which contributions dominate the variation of the span with θ. In Fig. 7 are the contributions to the spans from calculations for various PbI_6^{4-} structures as a function of the deviation from octahedral symmetry. As can be seen, over the range of deviations out to 12°, the diamagnetic contribution to the span is very nearly zero, so this component contributes very little to the overall span. The absolute magnitudes of the spin–orbit and paramagnetic contributions, on the other hand, increase as the deviation from octahedral symmetry becomes larger, with the paramagnetic contribution being more sensitive to the deviation than the spin–orbit contribution. Neither the spin–orbit nor the paramagnetic contribution is linear in the deviation, which suggests that the observed total span is comprised of partially offsetting contributions from these two components.

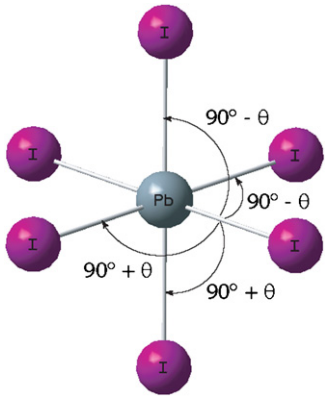

Fig. 5. The PbI_6^{4-} fragment representing the local environment of a Pb nucleus in a PbI_2 crystal. The structure of the fragment is a rhombohedrally distorted octahedron possessing a single threefold rotoinversion axis. It has six equal Pb–I distances, r_{Pb-I}, six I–Pb–I angles that are less than 90° by a deviation θ, and six I–Pb–I angles that are greater than 90° by the same deviation. This angle, θ, is a measure of the deviation of the structure from octahedral symmetry.

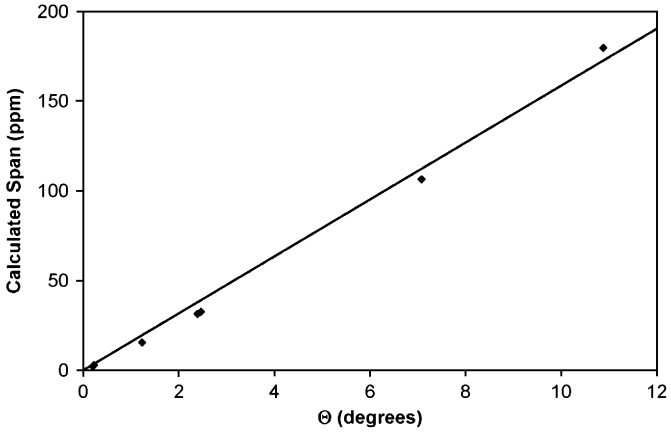

Fig. 6. The calculated spans of PbI_6^{4-} model cluster versus the deviation from octahedral symmetry, θ.

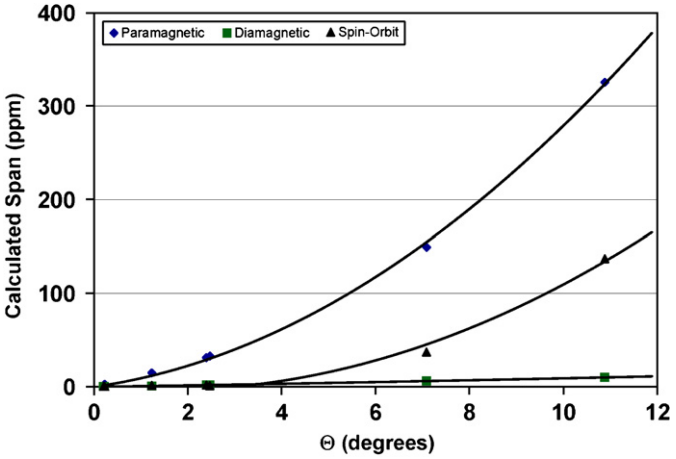

Fig. 7. The calculated paramagnetic (◆), diamagnetic (■) and spin–orbit (▲) contributions to the span of PbI_6^{4-} model cluster versus the deviation from octahedral symmetry, θ.

4. Conclusions

Cluster-based DFT-ZORA calculations of ^{207}Pb chemical shielding parameters reproduce experimental trends in the NMR parameters of the lead dihalides. The results, although reasonably accurate, are not as precise as measurements, with deviations of more than 100 ppm for some materials. The calculated values are sensitive to the parameters that define the structure, as seen in the variation of the parameters of PbI_6^{4-}. The present calculations suggest that the spin–orbit contributions to the isotropic chemical shifts of PbX_2 and PbX_4 are different in magnitude and in variation with anion partner. The results suggest that the opposite trends of chemical shift with anion partner observed experimentally for these two families of lead halides is a reflection of the difference in the spin–orbit contribution, and therefore reflects the significant s-type bonding in PbX_4, as compared to PbX_2.

Chemical-shift tensor properties such as the span and skew are also strongly affected by structure in the cluster models we have investigated. For PbI_6^{4-}, the paramagnetic contribution seems to have the greatest sensitivity to structure, with the spin–orbit contribution being less sensitive. The diamagnetic contribution to the span is very small and is only slightly dependent on structure. As these results demonstrate, the combination of calculations at this level of precision, or greater, with experimentally observed NMR parameters provides a detailed way to examine the effect of local environment on the electronic structure of heavy metal nuclei like lead.

Acknowledgments

CRD acknowledges the support of the National Science Foundation under Grant CHE-0411790. The computational part of this work was supported, in part, by the National Computational Science Alliance under CHE060075 (TeraGrid development project) and utilized the NCSA IBM pSeries 690. We thank the ADF team, Dr. Stan van Gisbergen and Dr. Erik van Lenthe for the providing prompt and efficient technical help with ADF-related computational problems.

References

[1] S. Aggarwal, A.M. Dhote, R. Ramesh, W.L. Warren, G.E. Pike, D. Dimos, M.V. Raymond, B.A. Tuttle, J.T. Evans Jr., Appl. Phys. Lett. 69 (1996) 2540–2541.
[2] P. Ekdunge, D. Simonsson, J. Electrochem. Soc. 132 (1985) 2521–2529.
[3] V.I. Birss, M.T. Shevalier, J. Electrochem. Soc. 137 (1990) 2643–2647.
[4] D.R. Lynam, L.G. Piantanida, J.F. Coles (Eds.), Environmental Lead, Academic Press, New York, 1981.
[5] J.O. Nriagu (Ed.), The Biogeochemistry of Lead in the Environment, Elsevier, New York, 1978.
[6] [a] A. Nolle, Z. Naturforsch. 32A (1977) 964–967;
[b] A. Nolle, Z. Naturforsch. 33 (1978) 666–671;
[c] A. Nolle, O. Lutz, Z. Phys. 36B (1980) 323–328.
[7] B.H. Suits, M. Nizam, M. Allavena, Y. Boutelier, D. White, J. Magn. Reson. 82 (1989) 441–453.
[8] J. B Grutzner, K. Stewart, R. Wasylishen, M. Lumsden, C. Dybowski, P.A. Beckmann, J. Am. Chem. Soc. 123 (2001) 7094–7100.
[9] [a] G. Neue, D. Barich, M. Smith, C. Dybowski, Solid State Nucl. Magn. Reson. 3 (1994) 115–119;
[b] G. Neue, C. Dybowski, M.L. Smith, M.A. Hepp, D.L. Perry, Solid State Nucl. Magn. Reson. 6 (1996) 241–249;
[c] S. Van Bramer, A. Glatfelter, S. Bai, C. Dybowski, G. Neue, Conc. Magn. Reson. 14 (2002) 365–387.
[10] C. Dybowski, M.L. Smith, M.A. Hepp, E.J. Gaffney, G. Neue, D.L. Perry, Appl. Spectrosc. 52 (1998) 426–429.
[11] G. Neue, C. Dybowski, Prog. Nucl. Magn. Reson. Spectrosc. 41 (2002) 153–170.
[12] F. Fayon, I. Farnan, C. Bessada, J. Coutures, D. Massiot, J.P. Coutures, J. Am. Chem. Soc. 119 (1997) 6837–6843.
[13] P. Zhao, S. Prasad, J. Huang, J. Shore, J.J. Fitzgerald, J. Phys. Chem. B 103 (1999) 10617–10626.
[14] D. Bussian, G. Harbison, Solid State Commun. 115 (2000) 95–98.
[15] G.G. Briand, A.D. Smith, G. Schatte, A.J. Rossini, R.W. Schurko, Inorg. Chem. 46 (2007) 8625–8637.
[16] S.K. Wolff, T. Ziegler, E. van Lenthe, E.J. Baerends, J. Chem. Phys. 110 (1999) 7689–7698.
[17] E. van Lenthe, E.J. Baerends, J.G.J. Snijders, Chem. Phys. 99 (1993) 4597–4610.
[18] T.M. Gilbert, T. Ziegler, J. Phys. Chem. A 103 (1999) 7535–7543.
[19] G. Schreckenbach, S.K. Wolff, T. Ziegler, J. Phys. Chem. A 104 (2000) 8244–8255.
[20] E.J. Baerends, J. Autschbach, A. Bérces, F.M. Bickelhaupt, C. Bo, P.L. de Boeij, P.M. Boerrigter, L. Cavallo, D.P. Chong, L. Deng, R.M. Dickson, D.E. Ellis, L. Fan, T.H. Fischer, C. Fonseca Guerra, S.J.A. van Gisbergen, J.A. Groeneveld, O.V. Gritsenko, M. Grüning, F.E. Harris, P. van den Hoek, C.R. Jacob, H. Jacobsen, L. Jensen, G. van Kessel, F. Kootstra, E. van Lenthe, D.A. McCormack, A. Michalak, J. Neugebauer, V.P. Osinga, S. Patchkovskii, P.H.T. Philipsen, D. Post, C.C. Pye, W. Ravenek, P. Ros, P.R.T. Schipper, G. Schreckenbach, J. G. Snijders, M. Solà, M. Swart, D. Swerhone, G. te Velde, P. Vernooijs, L. Versluis, L. Visscher, O. Visser, F. Wang, T.A. Wesolowski, E. van Wezenbeek, G. Wiesenekker, S.K. Wolff, T.K. Woo, A.L. Yakovlev, T. Ziegler, Amsterdam Density Functional Program (ADF), 2006.01.
[21] [a] G. Schreckenbach, T. Ziegler, J. Phys. Chem. 99 (1995) 606–611;
[b] G. Schreckenbach, T. Ziegler, Int. J. Quantum Chem. 60 (1996) 753–766;
[c] G. Schreckenbach, T. Ziegler, Int. J. Quantum Chem. 61 (1997) 899–918.
[22] S.K. Wolff, T. Ziegler, J. Chem. Phys. 109 (1998) 895–905.
[23] S.H. Vosko, L. Wilk, M. Nusair, Can. J. Phys. 58 (1980) 1200–1211.
[24] A.D. Becke, Phys. Rev. A 38 (1988) 3098–3100.
[25] J.P. Perdew, Phys. Rev. B 33 (1986) 8822–8824.
[26] The Inorganic Crystal Structure Database is copyrighted by the Fachinformationszentrum Karlsruhe and the National Institute of Standards and Technology. Information on the database is available at 〈http://icsdweb.fizkarlsruhe.de/〉.
[27] K.J. Ooms, K.W. Feindel, M.J. Willans, R.E. Wasylishen, J.V. Hanna, K.J. Pike, M.E. Smith, Solid State Nucl. Magn. Reson. 28 (2005) 125–134.
[28] T. Oyamada, T. Iijima, H. Kimura, Bull. Chem. Soc. Jpn. 44 (1971) 2638 (Pb–C = 2.238 Å).
[29] R.K. Harris, E.D. Becker, S.M. Cabral de Menezes, R. Goodfellow, P. Granger, Pure Appl. Chem. 73 (2001) 1795–1818.
[30] A. Rodriguez-Fortea, P. Alemany, T. Ziegler, J. Phys. Chem. A 103 (1999) 8288–8294.
[31] O. Dmitrenko, S. Bai, P.A. Beckmann, S.E. van Bramer, A.J. Vega, C. Dybowski, J. Phys. Chem. 112 (2008) 3046–3052.
[32] R.M. Hawk, R.R. Sharp, J. Chem. Phys. 60 (1974) 1009–1017.
[33] J.D. Kennedy, W. MacFarlane, G.S. Pyne, J. Chem. Soc. Dalton Trans. 23 (1977) 2332–2336.